Thioredoxin rod-derived cone viability factor protects against photooxidative retinal damage

G Elachouri, I Lee-Rivera, E Clérin, M Argentini, R Fridlich, F Blond, V Ferracane, Yingying Yang, W Raffelsberger, Jun Wan, et al.

Original Article

The thioredoxin RdCVFL protects against photo-oxidative retinal damage

Elachouri G[1,2,3]*, Lee-Rivera I[1,2,3]*, Clérin E[1,2,3], Argentini M[1,2,3], Fridlich R[1,2,3], Blond F[1,2,3], Ferracane V[1,2,3], Yang Y[1,2,3] , Raffelsberger W[4], Jun Wan[5], Bennett J[6], Sahel J-A[1,2,3], Zack DJ[1,2,3,5], Léveillard T **[1,2,3]

* these authors contribute equally to the work

** to whom correspondence should be addressed

[1] INSERM, U968, Paris, F-75012, France

[2] Sorbonne Universités, UPMC Univ Paris 06, UMR_S 968, Institut de la Vision, Paris, F-75012, France

[3] CNRS, UMR_7210, Paris, F-75012, France

[4] Université de Strasbourg CNRS - IGBMC UMR7104 - 1 rue Laurent Fries - BP10142 - F67404 Illkirch

[5] Departments of Ophthalmology, Molecular Biology and Genetics, Neuroscience, and Institute of Genetic Medicine, Johns Hopkins University, Baltimore, MD, USA

[6] Scheie Eye Institute, University of Pennsylvania, Philadelphia, PA, USA

Corresponding author:

Thierry Léveillard, Department of Genetics, Institut de la Vision, INSERM UMR-S 968, 17, rue Moreau, 75012 Paris, France.

Telephone: 33 1 53 46 25 48; Fax: 33 1 53 46 25 02

E-mail: thierry.leveillard@inserm.fr

Running title: Photo-oxidative RdCVF

Abstract

Rod-derived Cone Viability Factor (RdCVF) is a trophic factor of the thioredoxins family that promotes the survival of cone photoreceptors. It is encoded by the nucleoredoxin-like gene 1 *Nxnl1* which also encodes by alternative splicing a long form of RdCVF (RdCVFL), a thioredoxin enzyme that interacts with TAU. The known role of thioredoxins in the defense mechanism against oxidative damage led us to examine the retinal phenotype of the *Nxnl1-/-* mice exposed to photo-oxidative stress. Here we found that, in contrast to wild-type mice, the rod photoreceptors of *Nxnl1-/-* mice are more sensitive to light after exposure to 1,700 or 2,500 lx. The delivery of RdCVF by AAV to mice deficient of *Nxnl1-/-* protects rods photoreceptors from light damage. Interestingly, the RdCVF2L protein, encoded by the paralog gene *Nxnl2*, is able to reduce TAU phosphorylation, as does RdCVFL, but does not protect the rod from light damage. Our result shows that the *Nxnl1* gene, through the thioredoxin RdCVFL, is part of an endogenous defense mechanism against photo-oxidative stress that is likely of great importance for human vision.

Introduction

The rate of oxygen metabolism is inversely correlated to life-span [1,2]. During the life of aerobic organisms, reactive oxygen species (ROS), which are formed *in situ* in response to oxygen metabolism, can cause various forms of tissue damage. In order to reduce the damaging effect of ROS on cellular macromolecules, the redox potential of the cell is carefully regulated. Contributing to such homeostasis, aerobic organisms have developed a number of antioxidant systems, and among these are those mediated by superoxide dismutase, catalase and the thioredoxin proteins [3]. Thioredoxin 1 (TXN), the founder of the thioredoxin family of proteins, is a 12 kDa protein with a redox active disulfide/dithiol group within its conserved active-site sequence CGPC. Reduced TXN catalyses the reduction of disulfide bounds in many target proteins, and oxidized TXN is reversibly reduced by the action of thioredoxin reductase and NADPH [4].

Retinal photoreceptor (PR) cells are particularly prone to oxidative damage because of their high consumption of oxygen, their high proportion of polyunsaturated fatty acids, and the capture of energetic photons from visible light by opsin molecules encased in their outer segment (OS): rhodopsin in rods and cone-opsins in cones [5]. TXNs have been implicated in promoting PR health and function in this highly oxidizing environment. Transgenic over-expression of TXN protects PRs against photo-oxidative damage [6] and up-regulation of TXN via the nuclear factor erythroid 2-related factor 2 (NRF2)-antioxidant response elicits an endogenous neuro-protective mechanism [7]. TXN plays an important role in maintaining a reducing environment in living cells and prevents apoptosis by sequestering the MAP kinase ASK1 under normoxic conditions [8,9].

Nxnl1 was identified in a high content screen for secreted factors promoting cone survival [10]. *Nxnl1* encodes two protein products by alternative splicing [11]. One, rod-derived cone viability factor (RdCVF) which results from intron retention, is a truncated thioredoxin

protein that lacks thioredoxin enzymatic activity. RdCVF slows down secondary cone degeneration in two genetically distinct rodent models of the inherited retinal degeneration retinitis pigmentosa (RP) [12,13]. The other, RdCVFL, generated by splicing of intron 1, exhibits thioredoxin enzymatic activity [14]. The retina of the *Nxnl1-/-* mice displays evidence of increased oxidative damage in normoxic conditions, and cone function is altered when the animals are raised in 75% oxygen [15]. As demonstrated for its paralogue *Nxnl2*, *Nxnl1* is probably bifunctional, with one product being a trophic factor and the second, a thioredoxin protein that increases the length of photoreceptor outer segments of the *Nxnl2-/-* mouse [16]. *In vitro*, RdCVFL protects cones against UV-damage, [17,18]. We found that RdCVFL interacts with the microtubule-associated protein TAU and protects it from oxidative damage [19]. The aggregation of TAU in the *Nxnl1-/-* retina is most likely linked to the progressive rod degeneration in that model [15].

In the retina, ROS are produced by light exposure and their concentration is increased in conditions of elevated blood oxygen [20,21]. Light-induced damage primarily affects rods [22]. These neurons discern dim light (scotopic vision) and are very sensitive to light within the maximum absorption spectra of their visual pigment, rhodopsin [23]. Rod degeneration in the first phase of RP is triggered by mutations in more than 50 different genes [24] and results in an increase in oxygen tension, which in turn affects the cones [25,26]. Taken together, these results suggest that RdCVFL is involved in the defense mechanism against light-induced oxidative injury on photoreceptors, rods and cones, while RdCVF protects cones.

We show here that the rods of the *Nxnl1-/-* mouse are more susceptible to photo-oxidative damage. We also demonstrate that virally mediated re-expression of thioredoxin RdCVFL in the *Nxnl1* null mouse protects rods against light induced damage.

Materials and Methods

Animals

All procedures adhered to the ARVO statement for the use of animals in ophthalmic and vision research and have been approval by the Darwin ethic committee (Ce5/2010/008). Animals, males and females in equal proportion, were raised under 12 h, 50 lux (lx) / 12 h, dark cycle and given *ad-libitum* access to food and water. Mice used were 11-16 weeks of age. *Nxnl1-/-* and *Nxnl2-/-* mice were generated on a pure BALB/c background [15,16].

Light Illumination

Mice were first dark adapted 16 h prior to light exposure. They were exposed to a regulated amount of light, generated by cool, white fluorescent lamps, with animals placed in aluminum foil-wrapped polycarbonate cages (one mouse per cage) for 1 hr. The mice then recovered for 24 h in the dark. The temperature was monitored not to be above 25°C. 0 lx corresponds to animals left in the dark whilst their littermates were exposed. Beyond 24 h, mice were returned to 12 h light/dark cycles of 50 lx.

Outer nuclear layer measurement

Animals were anesthetized 10 d after exposure with ketamine (160 mg/kg)-/-xylazine (32 mg/kg) and immediately perfused with 2.5 % glutharaldehyde and 2 % formaldehyde in phosphate buffered saline (PBS). Eyes were enucleated and incubated in fixative overnight. Lenses were removed and eyecups washed 5 times in 5 % sucrose, fixed for 1 h in 2 % osmium tetroxide and embedded in epoxy resin. Sections of 1 µm thick were made along the sagittal axis at the optic nerve level and stained with 1 % toluidine blue. Measurements of the outer nuclear layer (ONL) thickness were made on one section from each mouse as described [27]. Briefly, in each of the dorsal (superior) and ventral (inferior) hemispheres, ONL thickness was measured in nine sets of three measurements each (27 measurements for each hemisphere). The first sets were, centered 250 µm from the optic nerve head (ONH) and subsequent sets were

located more peripherally. Within each 250 µm position, three measurements were made equidistant each other by 50 µm. Those 54 measurements cover the entire retinal surface. Data were plotted as spidergrams from 6 animals for each condition.

Quantitative RT-PCR

QRT-PCR was performed according to Léveillard *et al.* [10]. RdCVF forward 5'-ATGGCATCTCTCTTCTCTGGACG-3' and reverse 3'-CCTCACCTCCTCAGTTCATC ATGG-5'; RdCVFL forward 5'-GCAACAGGACCTCTTCCTCA-3' and reverse 3'-CCAGACGCTGGATCTCCTC-5'; *Rps6* forward 5'-AAGCTCCGCACCTTCTATA-3' and reverse 3'-ACTCTGCCATGGGTCAGAAC-5'. The expression of *Rps6* (ribosomal protein S6) was used for normalization.

Production and delivery of the AAV constructs to the *Nxnl1*-/- mouse retina

The adeno-associated viral vector (AAV)2/8-RdCVFL, AAV2/8-RdCVF2L and AAV2/8-GFP were generated as described in Jaillard et al. [16]. Animals were anesthetized, and sub-retinal injections were performed with 1 µl of AAV2/8-RdCVFL, AAV2/8-RdCVF2L or AAV2/8-GFP at 3.10^{12} genome copies (gc/ml) into the right eye at 2 months old.

Optical coherence tomography (OCT)

Treated mice at the age of 3 months were anesthetized and pupils were dilated as described above. Eye dehydration was prevented by regular instillation of sodium chloride drops. OCT images were recorded for both eyes using a spectral domain ophthalmic imaging system (Spectral domain Optical coherence tomography, OCT, Bioptigen 840nm HHP, Bioptigen, North Carolina USA). We performed rectangular scans consisting of a 1.4 mm by 1.4 mm perimeter with 1000 A-scans per B-scan with a total B-scan amount of 100. Scans were obtained first while centered on the optic nerve, and then with the nerve displaced superiorly/inferiorly. OCT scans were exported from InVivoVue as AVI files. These files were loaded into ImageJ (version 1.47, National Institutes of Health, Bethesda, MD) where they

were registered using the Stackreg plug-in. Outer nuclear layer thickness was measured using in the whole eye area every 100 µm and the thicknes of each point was averaged for each treated, AAV2/8-GFP, AAV2/8-RdCVFL and AAV2/8-RdCVF2L (n = 6).

Transmission Electron Microscopy

Animals were sacrificed 24 h after light exposure. The eye cups were fixed in 2.5 % glutharaldehyde at room temperature for 2 h, washed overnight and post-fixed in osmium tetraoxide 1 % for 1 h at room temperature. Samples were washed in Ringer-Krebs buffer (140 mM NaCl; 4.5 mM KCl, 2.2 mM $CaCl_2$, 12 mM $MgSO_4$, 12 mM $NaHCO_3$, 0.44 mM KH_2PO_4, 5.55 mM Glucose, pH 7.4) followed by dehydration in graded ethanol and acetone. Samples were embedded in epoxy resin and ultrathin sections (~500 nm) were cut and stained with uranyl acetate and Pb-citrate and observed using electron microscopy (Met Zeiss 912, at 80 kV).

TUNEL Assay

Mice were sacrificed 24 h after irradiation, enucleated and the centre of the cornea was removed for the penetration of fixative solution (4 % paraformaldehyde in PBS) overnight at 4°C. The tissues were incubated successively in 10 %, 20 % and 30 % sucrose at 4°C and embedded in optimal cutting temperature (OCT, Sakura Finetek) medium. Terminal deoxynucleotidyl transferase-mediated biotinylated dUTP nick end labeling (TUNEL) was performed using the *in situ* cell death detection kit (Roche) on 10 µm sections.

Cell death quantification

Mice were sacrificed 6-72 h after irradiation. Apoptosis was quantified with a cell death detection ELISA assay (Roche) which quantifies the soluble mono- and oligo-nucleosomes released in the cell lysate as a function of apoptosis [28]. 6 to 72 h after exposure, pairs of retinas were homogenized with a polytron tissue grinder in 400 µl of the manufacturer's lysis buffer

(Roche). The lysate was centrifuged at 200 g for 10 min at room temperature and 20 µl of a 1/5 dilution of the supernatant were used per assay.

Western blotting

Western blotting method is described in Fridlich *et al.* [19]. For RdCVF, novel antibodies raised against the epitope peptide IRNNSDQDEVETEAELSRRLEN corresponding to RdCVF-N in Léveillard *et al.* [10] was used. Briefly, Nxnl1+/+ and Nxnl1-/- mice were sacrificed, enucleated and the neural retinas were dissected, sonicated twice 10 s on ice in RIPA buffer in the presence of a cocktail of proteinase inhibitors (P2714, Sigma). After 30 min on ice, the extracts were centrifuged 5 min at 12,000 rpm at 4°C and 30 µg of the supernatant, the whole cell extracted were loaded on a Laemmli gel and transferred to a 0.22 µm nitrocellulose (Biorad). After saturation, the membranes were incubated with rabbit polyclonal anti-RdCVF-N (1/5,000), mouse monoclonal anti-phospho-TAU (AT8 Innogenetics, 1/500) and anti-ATB (C4 Millipore, 1/10,000) ON at 4°C. The western blots were revealed with anti-rabbit IgG coupled to peroxidase (Jackson Immunoresearch, 1/15,000)."

RNA purification

Animals were sacrificed by cervical dislocation. The neural retina was dissected free of RPE and RNAs were purified using RNeasy purification kit (Qiagen).

Statistics

Statistical analyses were performed using one-way ANOVA followed by Bonferroni correction. For two sample comparisons, a Student's t-test assuming unequal variances and combined with a Bayes shrinkage approach was applied to reduce the number of false positives at low intra-replicate variance. Data were expressed as the mean +/- the standard error of the mean (SEM). In the figures, significances are indicated by * if $p < 0.05$, ** < 0.01 and *** < 0.001.

Results

The *Nxnl1-/-* retina is more sensitive to photo-oxidative damage.

We examined the susceptibility of the *Nxnl1* knockout mouse retina to photo-oxidative damage. As a first assessment, three month-old *Nxnl1-/-* and *Nxnl1+/+* control mice (isogenic on BALB/c background) were exposed to either 1,700, 2,500 or 5,000 lx for 1 hour (h), sacrificed 10 days (d) later, and then their outer nuclear layer (ONL) thickness was measured. The ONL thickness is a good surrogate marker for the relative number of rods as rods constitute 97% of the cells in the mouse ONL [29,30]. The ONL, measured over the dorso-ventral axis, was found to be thinner in the *Nxnl1-/-* animals as compared to controls in dark reared condition (0 lx, Fig. 1A and 1E), as previously described [15]. After exposure to 1,700 lx, the ONL of the *Nxnl1-/-* demonstrated thinning compared to control, particularly in the ventral part of the retina (Fig. 1B). This is visible on retinal section (Fig. 1F). At this low dose, the thinning of the ONL was specific to the *Nxnl1-/-* mouse. With the higher dose of 2,500 lx, reduction of ONL thickness was observed for both genotypes, but the reduction was significantly more pronounced for the *Nxnl1-/-* mouse (Fig. 1C and 1G). At 5,000 lx, both genotypes exhibited marked damage to the ONL, suggesting that this dose of light is toxic and too high for study of the photoreceptor protective role of *Nxnl1* (Fig. 1D and 1H).

To confirm that the increased susceptibility of *Nxnl1-/-* mice to phototoxic injury results in excess damage to PRs, we analyzed the morphology of the retinas shortly after light exposure using transmission electron microscopy (Fig. 2). PRs undergo ultrastructural changes 24 h after light exposure, including pyknotic nuclei resulting from chromatin condensation [31]. PRs of the *Nxnl1-/-* mouse look more damaged than those of *Nxnl1+/+* mouse, even in the absence of light [15]. After illumination to 2,500 lx, *Nxnl1-/-* OSs and cell bodies in the ONL are swollen, the condensed chromatin is distinctly visible only in the *Nxnl1-/-* retina.

Photoreceptor apoptosis in the *Nxnl1-/-* mice after light exposure.

To characterize the apoptosis process, we exposed *Nxnl1-/-* and *Nxnl1+/+* mice to 1,700 and 2,500 for 1 h and examined internucleosomal DNA cleavage 24 h after. We used two independent investigation methods: *in situ*, using TUNEL assay and a quantitative ELISA assay, based on the detection of free nucleosomes in retinal extracts [32]. An increase in the number of TUNEL-positive cells was observed in the ONL with only a few TUNEL-positive cells being observed in the inner retina after light exposure (Fig. 3A). No differences between the *Nxnl1-/-* and control mice (*Nxnl1+/+*) at 1,700 and 2,500 lx could be observed at 24 h even though the retina is more damaged 10 days later. This correlated with the number of released nucleosomes, suggesting that the extent of apoptosis is similar for both genotypes 24 h after exposure (Fig. 3B). In the kinetic analysis at 2,500 lx, DNA fragmentation peaks at 24 h with similar amplitude for both genotypes (Fig. 3C). A significant increase of the nucleosome enrichment factor was observed for the *Nxnl1-/-* retinas at 72 h in agreement with its higher light susceptibility. This suggests the occurrence of a second wave of apoptosis in the absence of *Nxnl1*.

TAU phosphorylation in response to light.

The degeneration of rods occurring in an aged-dependant manner in the *Nxnl1-/- retina* is correlated to the aggregation of TAU [15]. The hyperphosphorylation of TAU and its aggregation are hallmarks of Alzheimer's disease [33]. We therefore analyzed the effect of light on TAU phosphorylation 24 h after exposure. We confirmed that TAU is hyperphosphorylated in the retina of the *Nxnl1-/-* mouse compared to control under normal light conditions (50 lx) (Fig. 4A). However, for animals raised in the dark (0 lx, or dark reared), phosphorylation was the same of both genotypes suggesting an effect of light on TAU phosphorylation in the retina. Light exposure decreases TAU phosphorylation in the *Nxnl1+/+* retinas (Fig. 4A and 4B). It

was reported that TAU is dephosphorylated prior to apoptosis mediated by UV light by the trimeric phosphatase PP2A, through the PPP2R2A regulatory subunit [34,35]. Here, exposure of the *Nxnl1-/-* mouse to 2,500 lx did not induce TAU dephosphorylation, as observed in control. This suggests that the absence of RdCVFL impairs light-induced TAU dephosphorylation.

Light exposure decreases RdCVFL expression.

Although the consequence of light illumination on photoreceptors can be recorded 24 h and 10 days after exposure, the kinetics of photon capture are much faster [36]. We analyzed the expression of *Nxnl1* in the retina of *Nxnl1+/+* mice immediately after one hour exposure to 2,500 lx. Groups of three animals were either exposed to 2,500 lx or dark adapted and sacrificed immediately afterward. One of the eyes of each mouse was used to measure messenger RNA expression and the second eye was used to analyze protein expression. Light induces a decrease of both RdCVFL mRNA (Fig. 5A) and protein (Fig. 5B) expression. The concomitant increase in expression of the RdCVF mRNA suggests an effect of light on intron retention. The absolute values are non-statistically significant (Fig. 5A), but the difference in the ratio RdCVFL/RdCVF between the two conditions is significant (result not shown). We could not assess RdCVF expression at the protein level because the antibodies available for western blotting were unfortunately not sensitive enough to detect endogenous RdCVF protein (Fig. 5B).

The administration of RdCVFL by AAV protect *Nxnl1-/-* mice retina from light.

In order to validate the role of *Nxnl1* in retina protection from light, we utilized an adeno-associated recombinant viral AAV2/8 vector, which targets principally photoreceptors [37], to restore specifically RdCVFL expression, and separately to over-express RdCVF2L, in *Nxnl1-/-* mice. Two months old mice were treated by subretinal injection of RdCVFL,

RdCVF2L or GFP vector, subjected to light exposure 1 month latter, and analyzed 10 days later. The injection of AAV2/8-GFP resulted in the presence of fluorescence in the ocular fundus of the treated animals (Fig. 6A). Before sacrificing the animals, the thickness of the outer retina was measured using optical coherence tomography (OCT) [38] (Fig. 6B). We observed that the injection of AAV2/8-RdCVFL protects rod photoreceptors from damage induced by illumination at 2,500 lx (Fig. 6C). Over all the surface of the retina in a dorso-ventral optic section the thickness of the ONL is 24-33 µm as compared to 16-25 µm for the animals treated with AAV-GFP. The treatment of the *Nxnl1-/-* mice with RdCVF2L resulted in only a partial protection around the optic nerve even in the presence of endogenous *Nxnl2* suggesting a specific role of *Nxnl1*. After sacrificing the animals, we analyzed the phosphorylation au TAU in groups of three animals. A decrease in the phosphorylation of TAU of similar amplitude was observed both for animals treated with AAV2/8-RdCVFL and AAV2/8-RdCVF2L (Fig. 7).

Discussion:

The present study provides the first evidence that *Nxnl1* has an essential role in preventing photo-oxidative damage of the retina. The BALB/c eye is not pigmented and consequently is particularly susceptible to light damage [39]. The doses of light used to expose those non-pigmented mice for 1 h are within visual experience for diurnal animals: 1,000 lx corresponds to an overcast day and 10,000-130,000, to a sunny day (http://stjarnhimlen.se/comp/radfaq.html#10). Mice are nocturnal and are usually active at night even when raised in a 50 lx environment. Nevertheless, the negative effect of the disruption of the *Nxnl1* mouse after only 1 h of exposure to moderate intensity suggests that *NXNL1* in human might have similar protective role against photo-oxidative damage over decades of diurnal live. Even brief exposures to bright sunlight can produce a transient decline in visual function [40]. Military personnel exposed to tropical sunlight for several months during the second world war had retinal lesions resulting from light damage [41]. This may be relevant for several common retinal pathologies. Increased light exposure, especially to energetic short wave light (blue), is a risk factor for age-related macular degeneration (AMD) [42]. Cumulative oxidative damage in the retina can trigger an inflammatory cascade leading to PR degeneration. Specific complement factor H (*CFH*) haplotypes have been identified as major genetic risk factors for AMD [43]. CFH binds to malondialdehyde, a produced by lipid peroxidation, to inhibit complement cascade activation [44]. Interestingly, excessive lipid peroxidation, microglial activation, PRs dysfunction and death were also observed in the retina of the *Nxnl1-/-* mouse gene suggesting that it models this aspect of AMD pathophysiology [15].

The PR outer segment is the principal site of photochemical damage from exposure to excessive light both in humans and in animal models [45]. The daily renewal of rod and cone OSs has evolved to remove photo-chemically damaged macromolecules [46]. The first visible alteration induced by excessive light is the disruption of the disc membranes of rod OSs

associated with lipid peroxidation [47]. Subretinal injection of RdCVF in a dominant model of RP maintains the length of cone OSs [12]. RdCVF does not protect rods in that model or in a second model of recessive RP [10], but the causative mutations (*Rho* or *Pde6b*) are expressed specifically by rods and might be dominant over any protective effect of RdCVF. Light susceptibility of the *Nxnl1-/-* mouse results from the absence of the thioredoxin RdCVFL. Using AAV2/8 vectors that targets photoreceptors cells, we have shown that RdCVFL is able to protect rod photoreceptors of the *Nxnl1-/-* mouse against light damage (Fig. 6C). We also show that although the administration of AAV2/8-RdCVF2L prevents TAU phosphorylation to the same extend as RdCVFL (Fig. 7) it is significantly less effective than RdCVFL in protecting rods of the *Nxnl1-/-* mouse from light damage (Fig. 6C).

The relative absence of protection from light damage by RdCVF2L is providing insight into the mechanism explaining the absence of redundancy between the two genes. The CXXC thioredoxin active site of RdCVF2L was changed to a CXXS motif in the placental mammalian lineage, so that RdCVF2L is inactive as a thioredoxin [11]. The serine residue seems to be important for RdCVF2L's non-enzymatic function in placental mammals because it is strictly conserved in 21 placental mammalian species (Fig. S1). The absence of an active thioredoxin site, and hence thioredoxin activity, is most likely responsible for RdCVF2L's inability to complement for RdCVFL in terms of protecting rods against light damage. The possibility that the activity of ectopic RdCVF2L is masked by endogenous RdCVF2L is unlikely since the expression of *Nxnl2* is reduced in the *Nxnl1* retina [16]. Another indication of non-redundancy between the *Nxnl1* and *Nxnl2* genes in terms of photoreceptor survival is that while the ONL thins in an age dependant manner in the *Nxnl1-/-* mouse, a similar phenomenon was not observed in the *Nxnl2-/-* mouse [15,16]. We have shown previously that the thioredoxin RdCVFL interacts with TAU *in vitro* and that TAU is phosphorylated and aggregated in the *Nxnl1-/-* retina [19]. Our finding that RdCVF2L's ability to inhibit TAU phosphorylation is similar to that

of RdCVFL suggests that preventing TAU phosphorylation in and of itself is not sufficient to prevent rod loss and that other unidentified targets of the thioredoxin RdCVFL remain to be discovered.

Acknowledgements

We thank M. LaVail for ONL measurements, C. Grimm for light exposure, I. Renault for animals, A. Petrosian and V. Garnier for electron microscopy. O. Poch and R. Ripp for scientific support. We thank the phenotyping platform for OCT recording and the electron microscopy platform (IBPS/FR3631-CNRS-UPMC- et la Région Ile de France) for their work. This work was supported by Inserm, ANR, Région Ile de France, Labex LIFESENSES, CNRS and University de Strasbourg.

List of Abbreviations

AAV	Adeno-associated viral vector
AMD	Age-related macular degeneration
ANOVA	Analysis of variance
DAPI	4',6-diamidino-2-phenylindole
ELISA	Enzyme-linked immunosorbent assay
GO	Gene ontology
ONH	Optic nerve head
ONL	Outer nuclear layer
OS	Outer segments
PR	Photoreceptor
RdCVF	Rod-derived Cone Viability Factor
RPE	Retinal pigmented epithelium
ROS	Reactive oxygen species
RP	Retinitis pigmentosa
SEM	Standard error of the mean
TXN	Thioredoxin
TUNEL	Terminal deoxynucleotidyl transferase-mediated biotinylated dUTP nick end labeling

References

1 Rubner, M. *Volksernährungsfragen*. (Akademische Verlagsgesellschaft m.b.H., 1908).

2 Liochev, S. I. Reactive oxygen species and the free radical theory of aging. *Free radical biology & medicine* **60**, 1-4, doi:10.1016/j.freeradbiomed.2013.02.011 (2013).

3 Holmgren, A. Antioxidant function of thioredoxin and glutaredoxin systems. *Antioxidants & redox signaling* **2**, 811-820 (2000).

4 Lu, J. & Holmgren, A. The thioredoxin antioxidant system. *Free radical biology & medicine* **66**, 75-87, doi:10.1016/j.freeradbiomed.2013.07.036 (2014).

5 Ryan, S. J. *Retina*. 4th edn, (Elsevier Mosby, 2006).

6 Tanito, M. *et al.* Attenuation of retinal photooxidative damage in thioredoxin transgenic mice. *Neuroscience letters* **326**, 142-146 (2002).

7 Tanito, M., Agbaga, M. P. & Anderson, R. E. Upregulation of thioredoxin system via Nrf2-antioxidant responsive element pathway in adaptive-retinal neuroprotection in vivo and in vitro. *Free radical biology & medicine* **42**, 1838-1850, doi:10.1016/j.freeradbiomed.2007.03.018 (2007).

8 Saitoh, M. *et al.* Mammalian thioredoxin is a direct inhibitor of apoptosis signal-regulating kinase (ASK) 1. *The EMBO journal* **17**, 2596-2606 (1998).

9 Nadeau, P. J., Charette, S. J. & Landry, J. REDOX reaction at ASK1-Cys250 is essential for activation of JNK and induction of apoptosis. *Mol Biol Cell* **20**, 3628-3637 (2009).

10 Leveillard, T. *et al.* Identification and characterization of rod-derived cone viability factor. *Nature genetics* **36**, 755-759, doi:10.1038/ng1386 (2004).

11 Chalmel, F. *et al.* Rod-derived Cone Viability Factor-2 is a novel bifunctional-thioredoxin-like protein with therapeutic potential. *BMC Mol Biol* **8**, 74 (2007).

12 Yang, Y. *et al.* Functional cone rescue by RdCVF protein in a dominant model of retinitis pigmentosa. *Molecular therapy : the journal of the American Society of Gene Therapy* **17**, 787-795, doi:10.1038/mt.2009.28 (2009).

13 Leveillard, T. & Sahel, J. A. Rod-derived cone viability factor for treating blinding diseases: from clinic to redox signaling. *Sci Transl Med* **2**, 26ps16 (2010).

14 Brennan, L. A., Lee, W. & Kantorow, M. TXNL6 is a novel oxidative stress-induced reducing system for methionine sulfoxide reductase a repair of alpha-crystallin and cytochrome C in the eye lens. *PloS one* **5**, e15421, doi:10.1371/journal.pone.0015421 (2010).

15 Cronin, T. *et al.* The disruption of the rod-derived cone viability gene leads to photoreceptor dysfunction and susceptibility to oxidative stress. *Cell death and differentiation* **17**, 1199-1210 (2010).

16 Jaillard, C. *et al.* Nxnl2 splicing results in dual functions in neuronal cell survival and maintenance of cell integrity. *Human molecular genetics* **21**, 2298-2311, doi:10.1093/hmg/dds050 (2012).

17 Wang, X. W., Liou, Y. C., Ho, B. & Ding, J. L. An evolutionarily conserved 16-kDa thioredoxin-related protein is an antioxidant which regulates the NF-kappaB signaling pathway. *Free Radic Biol Med* **42**, 247-259 (2007).

18 Wang, X. W., Tan, B. Z., Sun, M., Ho, B. & Ding, J. L. Thioredoxin-like 6 protects retinal cell line from photooxidative damage by upregulating NF-kappaB activity. *Free Radic Biol Med* **45**, 336-344 (2008).

19 Fridlich, R. *et al.* The thioredoxin-like protein rod-derived cone viability factor (RdCVFL) interacts with TAU and inhibits its phosphorylation in the retina. *Mol Cell Proteomics* **8**, 1206-1218 (2009).

20 Mainster, M. A. & Turner, P. L. in *Retina* Vol. 2 (ed S. J. Ryan) 1857-1870 (2006).

21 Ruffolo, J. J., Jr., Ham, W. T., Jr., Mueller, H. A. & Millen, J. E. Photochemical lesions in the primate retina under conditions of elevated blood oxygen. *Invest Ophthalmol Vis Sci* **25**, 893-898 (1984).

22 Okano, K. *et al.* Retinal cone and rod photoreceptor cells exhibit differential susceptibility to light-induced damage. *J Neurochem* (2012).

23 Ham, W. T., Jr., Mueller, H. A. & Sliney, D. H. Retinal sensitivity to damage from short wavelength light. *Nature* **260**, 153-155 (1976).

24 Daiger, S. P., Sullivan, L. S. & Bowne, S. J. Genes and mutations causing retinitis pigmentosa. *Clinical genetics* **84**, 132-141, doi:10.1111/cge.12203 (2013).

25 Yu, D. Y. *et al.* Photoreceptor death, trophic factor expression, retinal oxygen status, and photoreceptor function in the P23H rat. *Invest Ophthalmol Vis Sci* **45**, 2013-2019 (2004).

26 Komeima, K., Rogers, B. S., Lu, L. & Campochiaro, P. A. Antioxidants reduce cone cell death in a model of retinitis pigmentosa. *Proceedings of the National Academy of Sciences of the United States of America* **103**, 11300-11305, doi:10.1073/pnas.0604056103 (2006).

27 Faktorovich, E. G., Steinberg, R. H., Yasumura, D., Matthes, M. T. & LaVail, M. M. Basic fibroblast growth factor and local injury protect photoreceptors from light damage in the rat. *J Neurosci* **12**, 3554-3567 (1992).

28 Leist, M. *et al.* Murine hepatocyte apoptosis induced in vitro and in vivo by TNF-alpha requires transcriptional arrest. *J Immunol* **153**, 1778-1788 (1994).

29 Walls, G. L. *The vertebrate eye and its adaptive radiation.* (Cranbrook Institute of Science, 1942).

30 Gerkema, M. P., Davies, W. I., Foster, R. G., Menaker, M. & Hut, R. A. The nocturnal bottleneck and the evolution of activity patterns in mammals. *Proceedings. Biological sciences / The Royal Society* **280**, 20130508, doi:10.1098/rspb.2013.0508 (2013).

31 Wenzel, A., Grimm, C., Samardzija, M. & Reme, C. E. Molecular mechanisms of light-induced photoreceptor apoptosis and neuroprotection for retinal degeneration. *Progress in retinal and eye research* **24**, 275-306 (2005).

32 Hingst, O. & Blottner, S. Quantification of apoptosis (programmed cell death) in mammalian testis by DNA-fragmentation ELISA. *Theriogenology* **44**, 313-319 (1995).

33 Iqbal, K., Liu, F., Gong, C. X., Alonso Adel, C. & Grundke-Iqbal, I. Mechanisms of tau-induced neurodegeneration. *Acta neuropathologica* **118**, 53-69, doi:10.1007/s00401-009-0486-3 (2009).

34 Mills, J. C., Lee, V. M. & Pittman, R. N. Activation of a PP2A-like phosphatase and dephosphorylation of tau protein characterize onset of the execution phase of apoptosis. *J Cell Sci* **111 (Pt 5)**, 625-636 (1998).

35 Xu, Y., Chen, Y., Zhang, P., Jeffrey, P. D. & Shi, Y. Structure of a protein phosphatase 2A holoenzyme: insights into B55-mediated Tau dephosphorylation. *Mol Cell* **31**, 873-885 (2008).

36 Lyubarsky, A. L. & Pugh, E. N., Jr. Recovery phase of the murine rod photoresponse reconstructed from electroretinographic recordings. *The Journal of neuroscience : the official journal of the Society for Neuroscience* **16**, 563-571 (1996).

37 Tan, M. H. *et al.* Gene therapy for retinitis pigmentosa and Leber congenital amaurosis caused by defects in AIPL1: effective rescue of mouse models of partial and complete Aipl1 deficiency using AAV2/2 and AAV2/8 vectors. *Human molecular genetics* **18**, 2099-2114, doi:10.1093/hmg/ddp133 (2009).

38 Berger, A. *et al.* Spectral-domain optical coherence tomography of the rodent eye: highlighting layers of the outer retina using signal averaging and comparison with histology. *PloS one* **9**, e96494, doi:10.1371/journal.pone.0096494 (2014).

39 Sanyal, S. & Zeilmaker, G. H. Retinal damage by constant light in chimaeric mice: implications for the protective role of melanin. *Experimental eye research* **46**, 731-743 (1988).

40 Gladstone, G. J. & Tasman, W. Solar retinitis after minimal exposure. *Archives of ophthalmology* **96**, 1368-1369 (1978).

41 Sliney, D. & Wolbarsht, M. Optical Hazards from the ambient environment. *Springer*, 187-215, doi:10.1007/978-1-4899-3596-0_6 (1980).

42 Kijlstra, A., Tian, Y., Kelly, E. R. & Berendschot, T. T. Lutein: more than just a filter for blue light. *Progress in retinal and eye research* **31**, 303-315, doi:10.1016/j.preteyeres.2012.03.002 (2012).

43 Klein, R. J. *et al.* Complement factor H polymorphism in age-related macular degeneration. *Science* **308**, 385-389, doi:10.1126/science.1109557 (2005).

44 Weismann, D. *et al.* Complement factor H binds malondialdehyde epitopes and protects from oxidative stress. *Nature* **478**, 76-81, doi:10.1038/nature10449 (2011).

45 Rattner, A. & Nathans, J. An evolutionary perspective on the photoreceptor damage response. *American journal of ophthalmology* **141**, 558-562, doi:10.1016/j.ajo.2005.10.045 (2006).

46 Young, R. W. The renewal of photoreceptor cell outer segments. *The Journal of cell biology* **33**, 61-72 (1967).

47 Lanum, J. The damaging effects of light on the retina. Empirical findings, theoretical and practical implications. *Survey of ophthalmology* **22**, 221-249 (1978).

Figure Legends

Figure 1: *Nxnl-/-* mice are more sensitive to light than its *Nxnl+/+* controls. Outer nuclear layer (ONL) thickness was measured in sagittal sections of the eye of *Nxnl1+/+* and *Nxnl1-/-* mice, 10 dafter exposure to 0 lx, or dark reared (A, E), 1,700 lx (B, F), 2,500 lx (C, G), and 5,000 lx (D, H) for 1 h. The spidergrams (A-D) represent measurements made along the retina. Light microscopy images illustrate the area with the most severe photoreceptor loss (E-H). Average (n = 5) and ± SEM were plotted; * $p<0.05$; ** $p<0.01$. ONH, optic nerve head. Scale bar, 25 µm.

Figure 2: Transmission electron microscopy images show that *Nxnl1-/-* photoreceptors are more damaged than those of *Nxnl1+/+* by light illumination. Retinas were prepared 24 h after 1 h exposure to 0 and 2,500. Outer segments (OS) disorganization and cell bodies in outer nuclear layer (ONL) present shrunken pyknotic nuclei (arrows). After illumination, *Nxnl1-/-* OS and the cell bodies in the ONL are swollen and condensed chromatin (*) in the nuclei is clearly visible. Scale bar, 5 µm. The panels on the left are lower magnifications for both genotypes. Scale bar, 10 µm.

Figure 3: Cell death is similarly induced in *Nxnl1-/-* and *Nxnl1+/+* retinas after light exposure. Cell death was determined 24 h after light exposure to 0, 1,700 and 2,500 lx using TUNEL assays. Representative images of the TUNEL assays (A). DNAse I treated slides were used as a positive control (C+). DAPI staining was performed after TUNEL labeling to localize the nuclear layers. Quantification of nucleosome release (nucleosome enrichment factor) from whole retina using ELISA assays (B). Kinetics of cell death induction after 2,500 lx exposure were plotted with data from the nucleosome release assays (C). The results are expressed as the mean ± SEM * $p<0.05$.

Figure 4: The phosphorylation of TAU protein is mediated by light. Mice were raised under normal conditions (50 lx), dark reared (0 lx) or exposed to 2,500 of light were analyzed for TAU phosphorylation in the retina by western blotting using pSer202+pThr205 antibody AT8 (A). The quantification was made from four independent experiments (B). The data were normalized to the expression of cytoplasmic actin (ACTB). Results are expressed as the mean ± SEM, * $p<0.05$; ** $p<0.01$ using Dunnett's test.

Figure 5. Light exposure decreases RdCVFL expression. The expression of *Nxnl1* in the *Nxnl1+/+* immediately after one hour exposure to 2,500 lx by RT-PCR (A) and western blotting (B). One of the eyes of each mouse was used to measure messenger RNA expression the second to analyze protein expression. Results are expressed as the mean ± SEM, * $p<0.05$.

Figure 6: Treatment of the *Nxnl1-/-* mouse by sub-retinal injection of recombinant AAV-RdCVFL reduces photoreceptor damage. Animals were injected in the subretinal space at 2 months of age with AAV2/8-GFP, AAV2/8-RdCVFL or AAV2/8-RdCVF2L. One month later, the animals were exposed to 2,500 lx and 10 days after, ONL thickness was measured by OCT. Ocular fundus from a GFP-treated animal (A). in red with white light and green with fluorescent light. Representative images of OCT sections at 0.5 mm from the optic nerve head. The thickness of the ONL is indicated (B). Graphic representation of the results (C). Results are expressed as the mean ± SEM, * $p<0.05$; ** $p<0.01$.

Figure 7: Treatment of the *Nxnl1-/-* mouse by sub-retinal injection of recombinant AAV-RdCVF and AAV-RdCVF2L reduces TAU phosphorylation. Western blotting analysis of groups of three treated animals ten days after exposure. P-TAU, antibody AT8 which

recognizes phosphorylated TAU. TAU5, total TAU, ACTB, actin (A). Quantitative analysis (B). Results are expressed as the mean ± SEM, * $p<0.05$; ** $p<0.01$.

Supplementary Figure S1: The thioredoxin active site CXXC of RdCVF2L was changed to a CXXS motif in the placental mammal lineage. Phylogenic representation constructed with 26 residues of RdCVF2L proteins centered on the thioredoxin active site CXXC using Clustal. The two cysteine residues are highlighted in blue and the serine residue in placental mammals in red. 1: Q5VZ03, 2: G1R065, 3: F7F4W5, 4: H2PSL7, 5: G3RVI9, 6: H2R6L8, 7: F6PZK8, 8: G1TU74, 9: G5C376, 10: D4A212, 11: E1BFN2, 12: L8IKZ1, 13: Q9D531, 14: H0WK68, 15: G7NEM5, 16: L5K9M3, 17: H0WB67, 18: M3WW70, 19: L9KL09, 20: G1L9B4, 21: M3YB03, 22: Q5PRB4, 23: Q6GQZ1, 24: G3PV59, 25: C1BXM1, 26: M4AGR9, 27: I3JL45, 28: H2UJI5, 29: H2LLK4, 30: B5XBV8, 31: Q4SQA3, 32: H3AX05, 33: G3VUR6, 34: F7DSV4, 35: K7GEY5, 36: R4GHS3, 37: U3KD57, 38: R7VPE3, 39: H0YQB7, 40: F6QDL8, 41: G1KSP9, 42: M7C6V9.

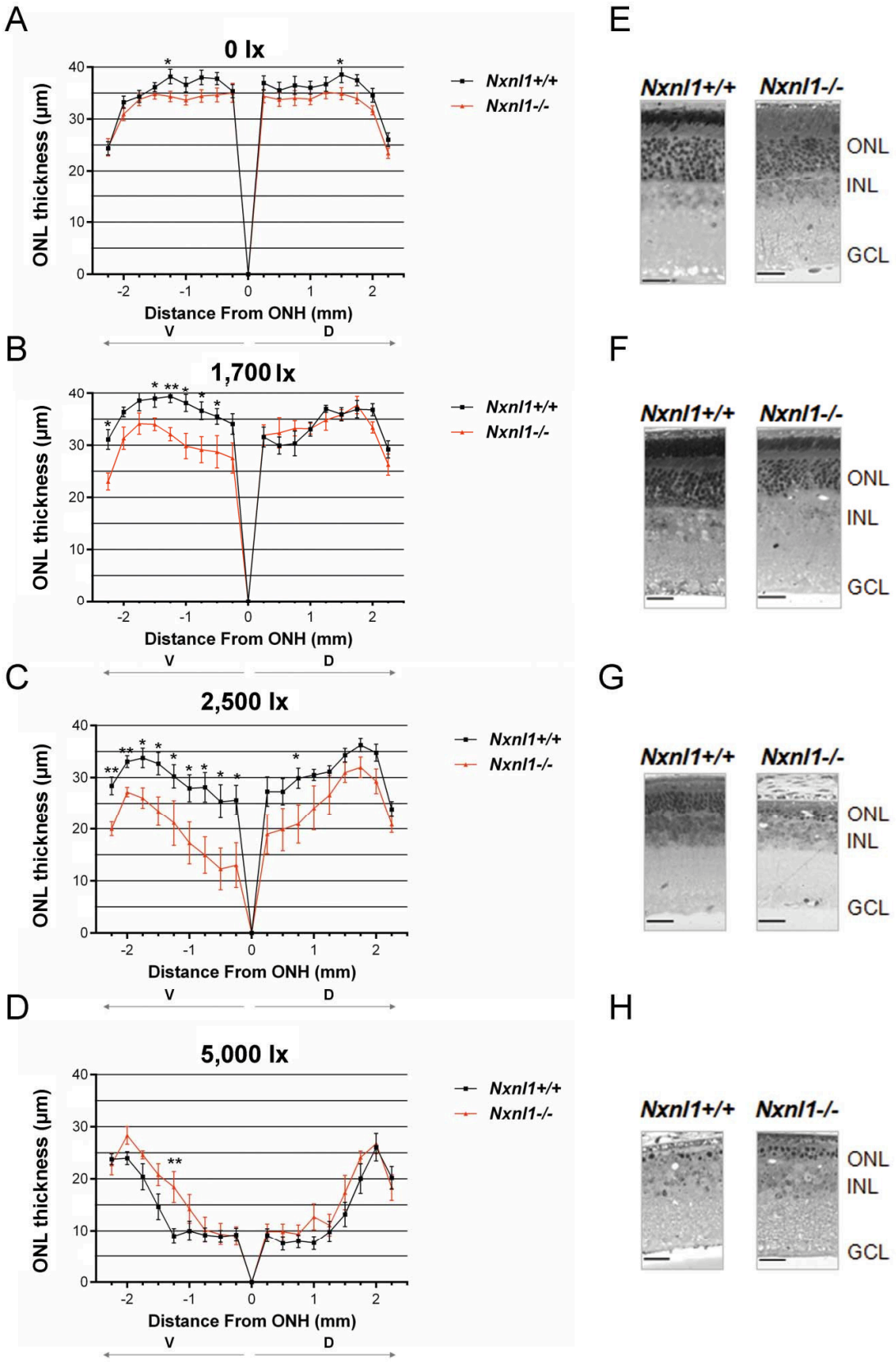

Figure 1

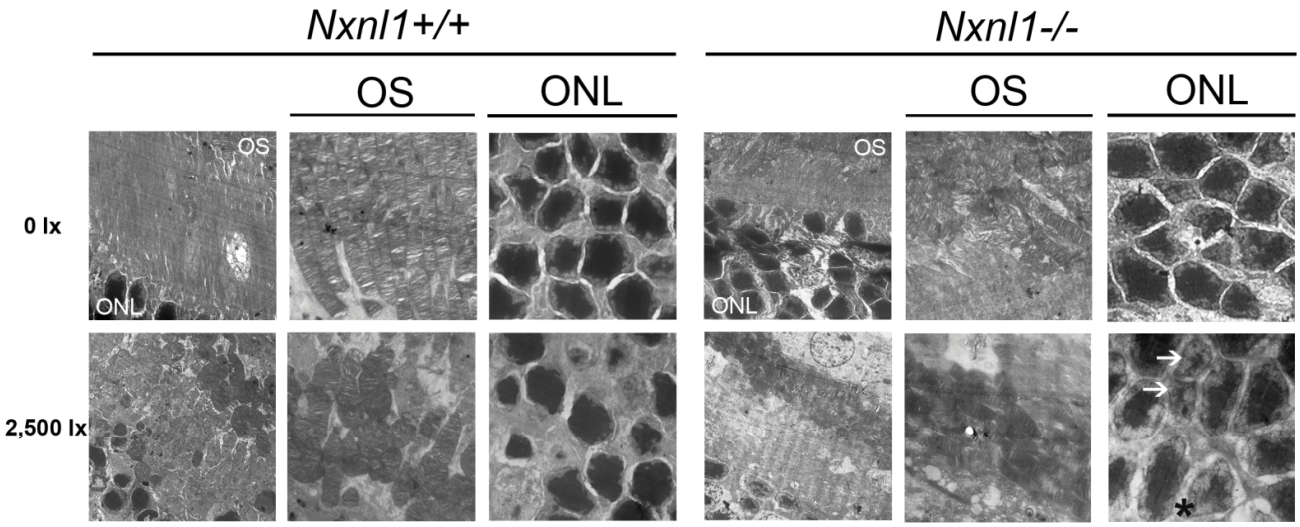

Figure 2

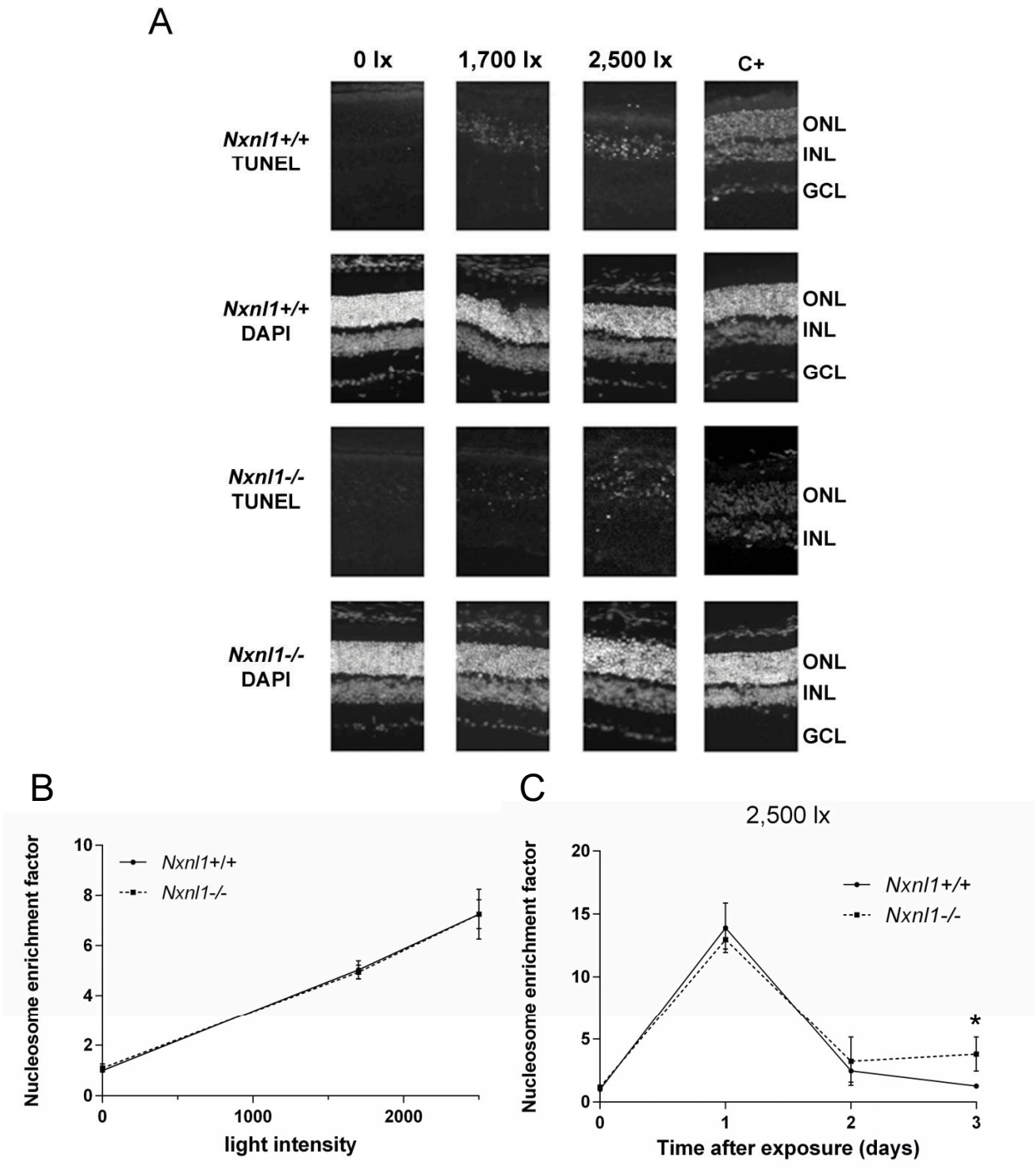

Figure 3

A

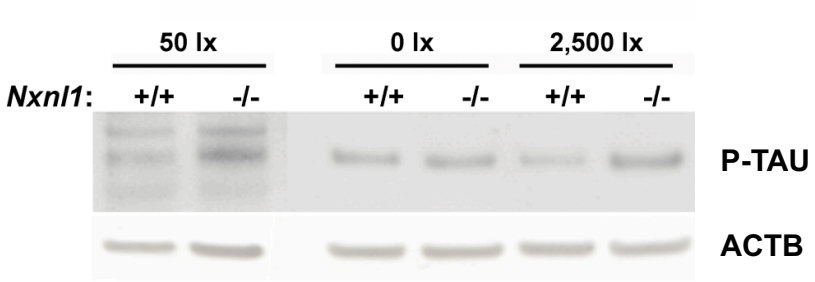

B

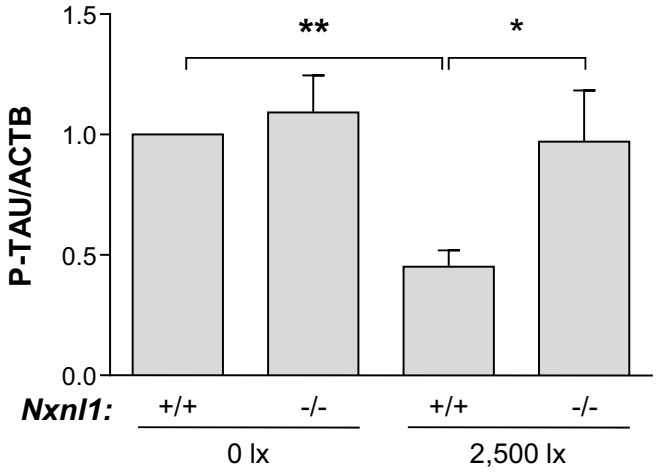

Figure 4

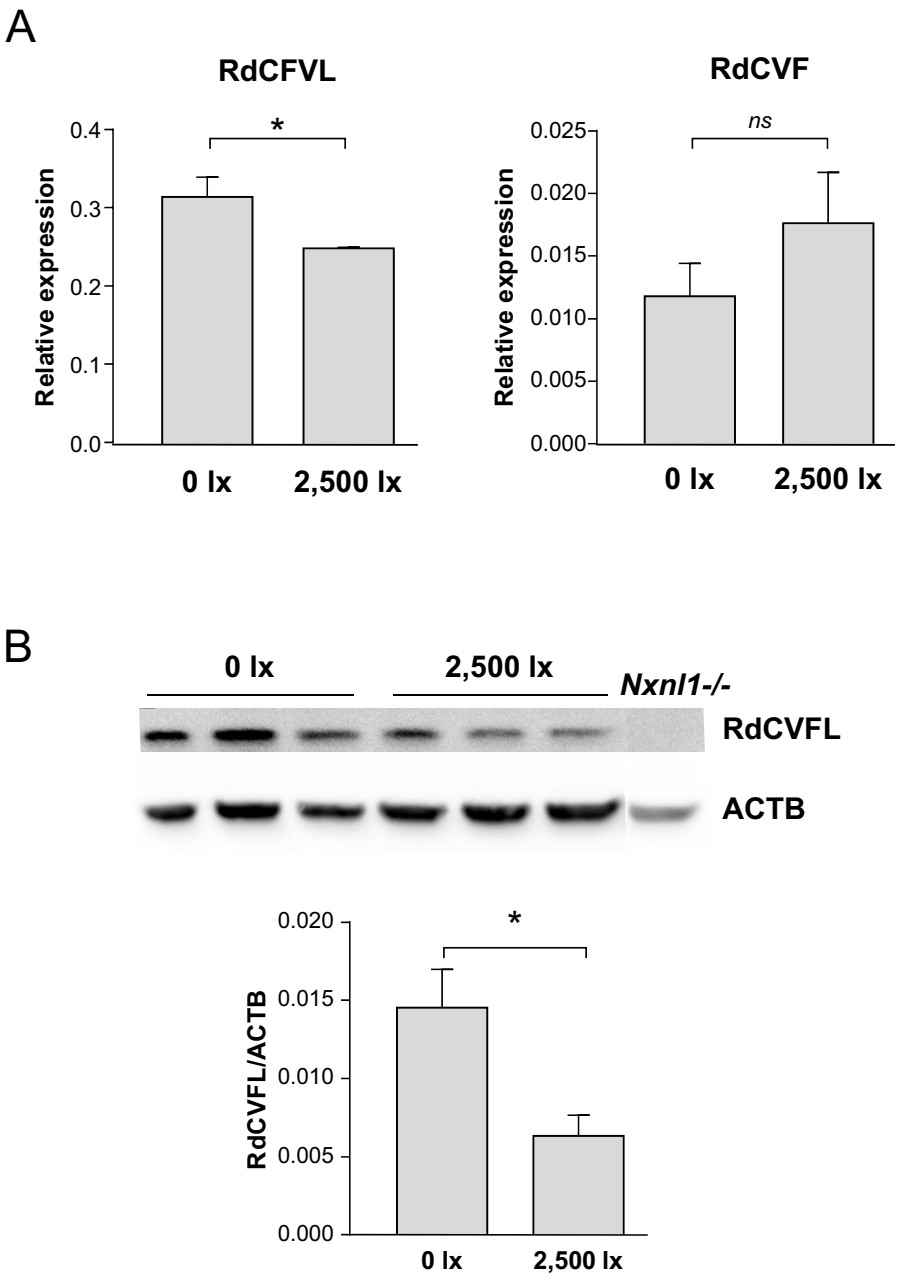

Figure 5

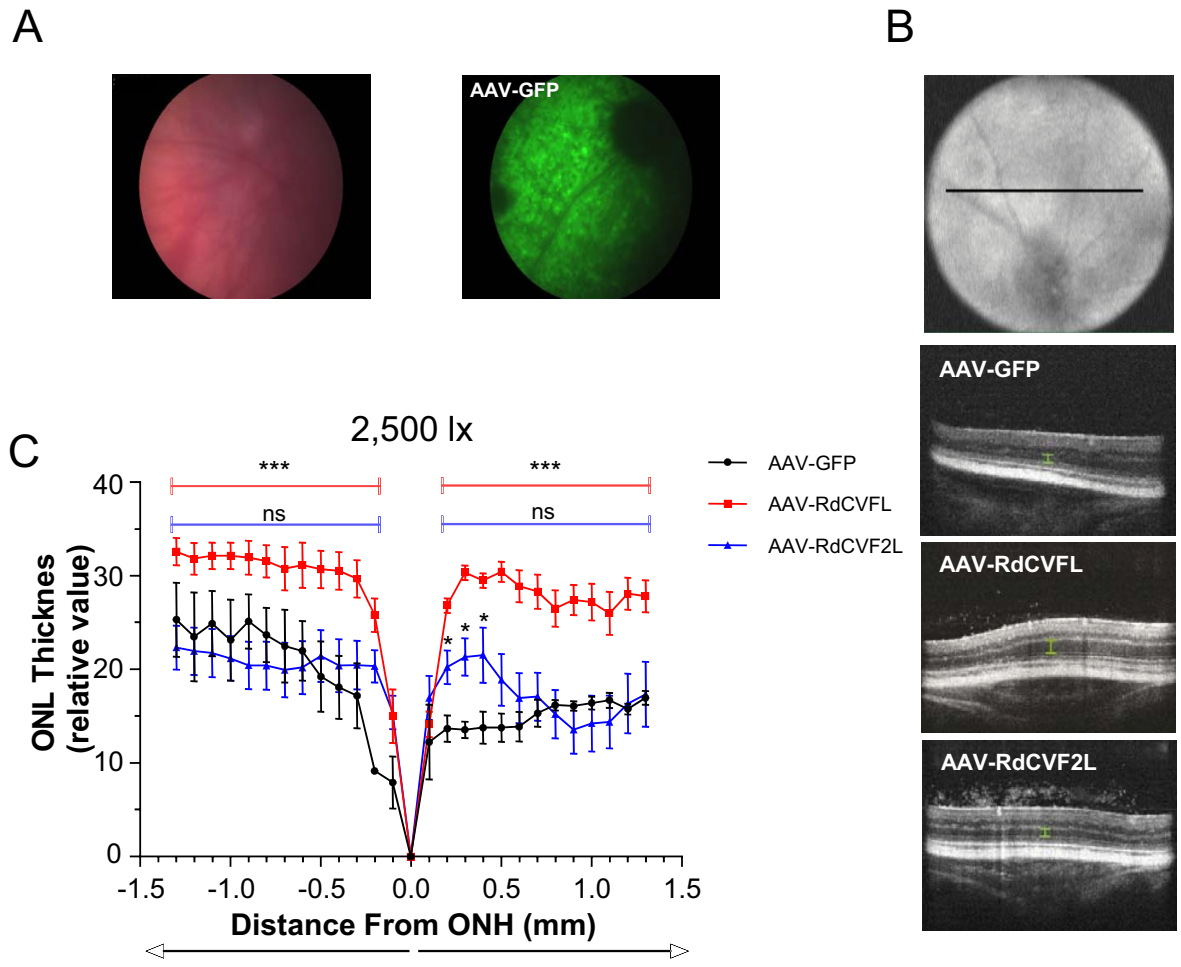

Figure 6

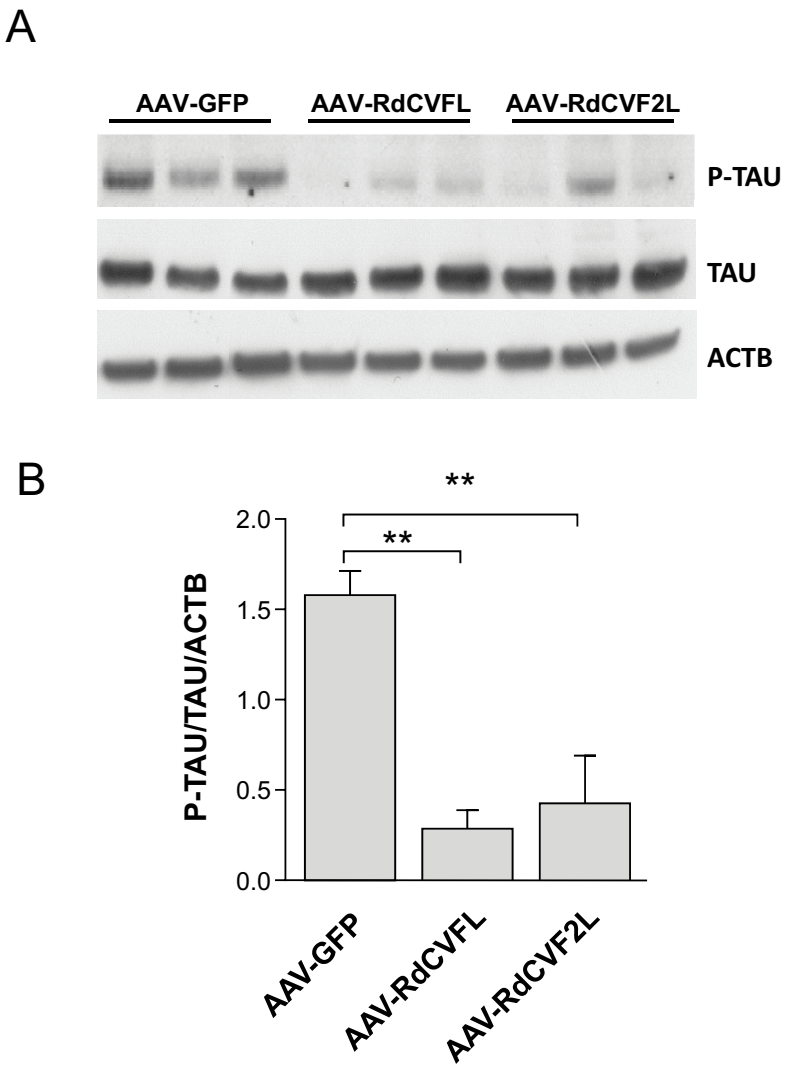

Figure 7